High-resolution retinal images obtained by deconvolution from wave-front sensing

Ignacio Iglesias and Pablo Artal

Laboratorio de Optica, Departamento de Física, Universidad de Murcia, Campus de Espinardo, 30071 Murcia, Spain

Received July 28, 2000

A new concept for high-resolution ophthalmoscopy is presented. The method is an alternative to the use of adaptive optics. It is based in deconvolving a retinal image from simultaneously acquired multiple ocular wave-front aberration and aberration-distorted fundus images. A computer simulation of the procedure using actual ocular wave-front aberration data that shows the validity of the method is first presented. Experimental results obtained from an artificial eye serve both to probe the method in a situation similar to the real eye and to introduce the required preprocessing of the retinal images. Finally, results from a real human retina are presented, and the potential of the technique is discussed. © 2000 Optical Society of America

OCIS codes: 330.0330, 330.4300, 100.0100, 100.1830.

Adaptive optics promises to increase the resolution of ophthalmoscopes by correcting the wave aberration (WA) of the eye.[1,2] However, the required technologies are not yet completely mature, and they have a high cost, limiting their use in clinical ophthalmic devices. As an alternative, the use of deconvolution techniques that use an ocular point spread function (PSF) was proposed,[3] although there are not yet any practical implementations of such techniques. In this Letter we present a method of obtaining high-resolution retinal images based on those ideas.

Among the numerous deconvolution methods reported in the literature, one that we found adequate for application in the eye is deconvolution from wave-front sensing, as proposed by Primot *et al.*[4] This method uses multiple WA data and simultaneously acquired degraded images to provide an ensemble maximum likelihood estimate of the undistorted image. The method was proved with simulated wave-front aberration induced by atmospheric turbulence. Assuming incoherent illumination, an estimation of the object can be obtained with the expression

$$o_e = \mathrm{FT}^{-1}[\langle I_i S_i^* \rangle / \langle S_i S_i^* \rangle], \tag{1}$$

where FT denotes Fourier transform, the angle brackets denote an average, and I_i and S_i are the Fourier transforms of degraded images and the instantaneous optical transfer function, respectively. The optical transfer function is computed from the measured WA obtained with a wave-front sensor. In addition to the benefits in noise reduction by averaging, an interesting property of Eq. (1) is that, assuming random aberrations, the averaging process fills zero-valued regions in the denominator, $\langle S_i S_i^* \rangle$, allowing one to avoid a common problem in inverse filtering of division by zero. Compared with WA induced by the atmosphere in astronomy, the WA of the human eye cannot be modeled as being produced solely by a random process. Instead, this WA can be regarded as a mixture of random and fixed components. The fixed aberration component is due to the approximately stable optical features of the eye optics. The variable (random) component is produced by significantly more rapidly varying processes such as accommodation microfluctuations, eye movements, and changes in the tear film, all with different characteristic frequencies.[5,6] To test whether WA of the human eye has enough variability for us to utilize this type of deconvolution method, a simulation was carried out. We used actual data on ocular WA recorded by a real-time (25-Hz) Hartmann–Shack (HS) apparatus.[6] The data were acquired by means of paralyzed accommodation, with the subject's head fixed by a bite-bar mount for 5 s. Despite the stable acquisition conditions, there were still important variations in the aberrations with time (see Ref. 6 for further details on the dynamics of ocular aberrations). Figure 1(a) shows an example of short exposure (PSF) computed from one of the ensemble WA's. We used the letters LOUM as the original object. By convolving this object with sequential PSF's and adding Gaussian noise to the normalized images, we computed a series of simulated degraded retinal images [Fig. 1(b), for example]. To reconstruct the object we applied Eq. (1), using a series of time-linked optical transfer

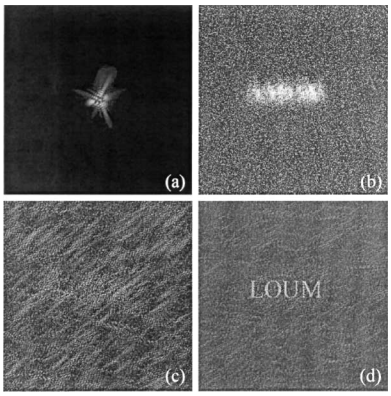

Fig. 1. Deconvolution of a simulated object (the letters LOUM) by use of real WA from a human eye: (a) Example of a PSF, (b) example of a distorted image, (c) and (d) results for 5 and 20 realizations, respectively. All images are 256 × 256 pixels.

0146-9592/00/241804-03$15.00/0

functions and distorted objects. A good estimate of the object was obtained in these realistic conditions with a relatively low number of samples.

After we showed the validity of the deconvolution algorithm in a computer simulation, a modified ophthalmoscope was built. Figure 2 shows a schematic diagram of the setup. An Ar^+ laser (514 nm) was used to illuminate an artificial eye consisting of a lens and a U.S. Air Force resolution chart located at the "retinal" surface. To produce incoherent illumination we used two independent rotating diffusers made from frosted glass, which permitted the CCD sensors to integrate different speckle patterns during the acquisition time. We use a lens system to collect the light emerging from the diffusers to illuminate an extended area of the resolution chart. After a second pass through lenses L_3 and L_2 and reflection in beam splitter BS_1, the light emerging from the chart was divided into two output channels by beam splitter BS_2. One of the beams was directed to a HS wave-front sensor and CCD_1, and the other beam was directed through lens L to CCD_2, which recorded images of the retina (in the artificial eye these images correspond to the resolution chart). A Badal system (mirrors M_1 and M_2 and lenses L_3 and L_2) allowed us to introduce or correct defocus. The two CCD's were synchronized with an electronic shutter, permitting simultaneous registration of HS and retinal images. To produce a fixed, relatively large WA, we tilted L_2 slightly. Variable aberrations were introduced in each frame by random displacement of the translation stage. Figure 3(a) shows one of the fundus (retinal) images obtained with a 300-ms exposure time and a 5-mm-diameter pupil. It can be seen that degradation occurs mostly for the vertical features. Also, there is residual speckle caused by the limit in the ability to decorrelate the speckle patterns of the system of rotating diffusers. Figure 3(b) shows a simultaneously acquired HS image. Each HS lenslet images the same structured object, forcing us to use a different type of processing than the center-of-mass-type algorithm commonly used to compute WA from HS images.[7] Since a HS image with an extended object as the source is the convolution of the paraxial image of the object produced by a lenslet with the image that a lenslet array with a point object source would generate, the main task is to find the coordinates where the lenslet images are centered. With the central lenslet image as the reference, the relative coordinates of the rest of the images correspond to the positions where the correlation between the reference image and the whole HS image reaches local maxima. First, the program searches for maxima in a correlation image computed with a fast Fourier transform algorithm that applies the correlation theorem. After a maximum is found, we use a square mask to exclude a secondary maximum in the area of the HS image associated with a lenslet. Although this approach is simple, the drawback is that the precise position of the autocorrelation maxima cannot be found, owing to fast Fourier transform windowing effects. To refine the coordinate estimates we sequentially shift the reference subimage by a few pixels from the previously found maximum positions and compute the spatial-domain cross correlation[8] between the reference subimage and the particular region in the HS image. Once the maxima are extracted, the geometry of the lenslet array is used to obtain a square reference grid that is centered with respect to the autocorrelation maximum of the HS central subimage. These data are used to obtain the WA. Notice that this procedure is not sensitive to the tip and tilt components, since the absolute position of the reference grid varies between

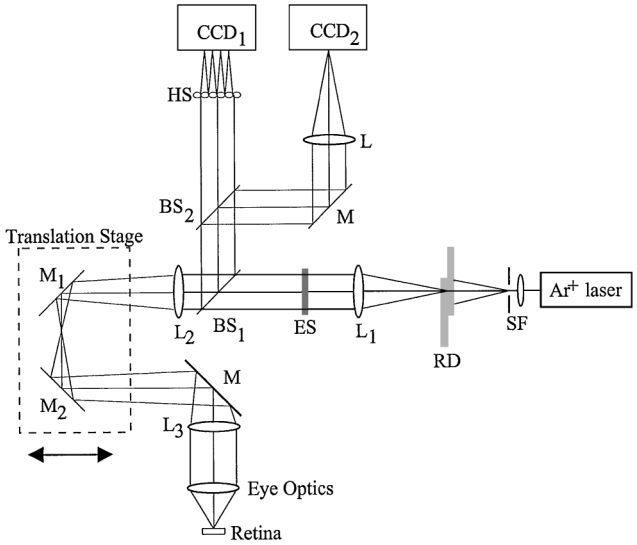

Fig. 2. Schematic of the experimental setup: CCD_1, CCD_2, cooled CCD sensors; HS, Hartmann–Shack microlens array; M_1, M_2 mirrors; L_1–L_3, L, lenses; BS_1, BS_2, beam splitters; SF, spatial filter; ES, electronic shutter; RD, system of rotating diffusers.

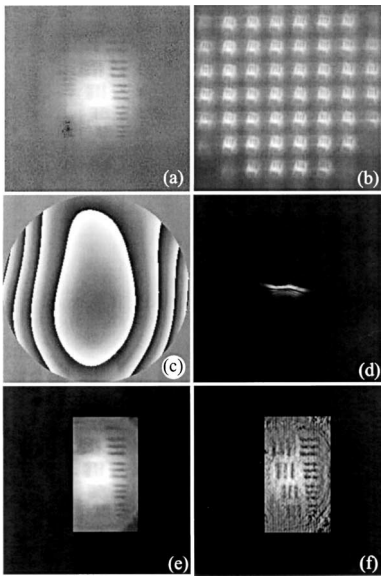

Fig. 3. Artificial eye experiment: (a) registered HS image (512 × 512 pixels), (b) simultaneously acquired "retinal" image, (c) example of a WA represented wrapped, (d) detail of the associated PSF. (e) and (f) average of 20 recentered "retinal" images and a deconvolved object, respectively (both 256 × 256 pixels). A mask is used in (e) and (f) to cover pixels without relevant information to improve visualization.

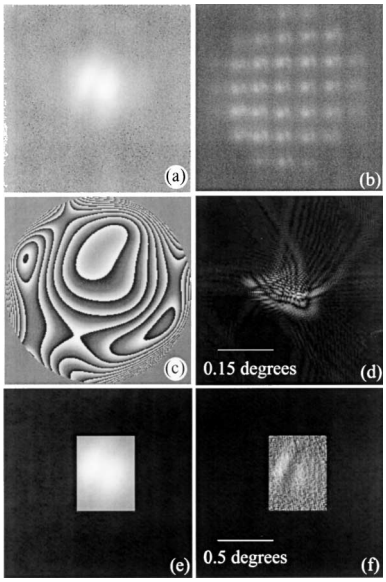

Fig. 4. Real eye experiment: (a) HS image (512 × 512 pixels), (b) simultaneously acquired fundus image, (c) example of a WA represented wrapped, (d) detail of the associated PSF, (e) and (f) average of nine recentered fundus images and a deconvolved object, respectively (both 256 × 256 pixels).

HS images. Figure 3 shows one of the computed WA's represented wrapped and the associated PSF. Since the retinal images are shifted by the tip and tilt components of the WA, the images must be recentered before deconvolution. The necessary displacements are calculated by a process similar to that used above to refine the coordinates of the lenslet images. A region of interest of the first ensemble image is selected as a reference. Then we compute cross correlations in the spatial domain between the ROI and the same area in each ensemble image, shifting the region of interest's position around its original coordinates each time. The coordinate values for which the cross correlations reach maxima are used to shift the fundus images. Figure 3(e) shows an average of 20 images after tip–tilt correction. It can be seen that there is noise reduction but no increase in resolution. Figure 3 shows an image that was deconvolved by use of 20 realizations ($i = 20$). There is a general improvement in the resolution of the more-degraded details. Only the central portion of the image is adequately recovered, indirectly indicating the isoplanatic patch of the system. Some artifacts are present. The source of these artifacts could be associated with the precision of the estimation of the PSF's, residual speckle in the fundus images, and noise.

We also applied the procedure described above to images recorded in a living human eye (one of the authors, P. Artal, served as the subject). Retinal images, subtending approximately 0.5°, were collected at 4° eccentricity with a 300-ms exposure and a 5-mm pupil diameter. Figure 4 shows an example of one of the nine retinal (fundus) images that were recorded, a simultaneously recorded HS image, and the associated WA and PSF. Figure 4 also shows an average of the selected fundus images after tip–tilt correction and a reconstructed image. In the reconstructed image more structure and small features appear; these features are only inferred in some of the individual images. To ensure that the gain was not artificial, we also carried out deconvolution, orienting the horizontal and vertical axes of the PSF's in the eight possible combinations of orthogonal directions. Improvement was found only with the orientation and scaling that were consistent with the present optical setup. Despite the additional sources of error compared with those in the artificial eye, and considering the smaller number of realizations used in the reconstruction, this result shows the potential of the procedure described here for use in the living eye.

Although many possible improvements can be incorporated in both the experimental setup and the data processing, we have shown in this Letter that one can successfully use joint information on degraded retinal images and the ocular wave front to improve the resolution of retinal images by use of deconvolution.

This research was supported by Dirección Generale de Enseñanza Superior-Spain grant PB97-1056. I. Iglesias's e-mail address is iic@um.es.

References

1. J. Liang, D. R. Williams, and D. T. Miller, J. Opt. Soc. Am. A **14,** 2884 (1997).
2. F. Vargas-Martin, P. Prieto, and P. Artal, J. Opt. Soc. Am. A **15,** 2552 (1998).
3. I. Iglesias, N. Lopez-Gil, and P. Artal, J. Opt. Soc. Am. A **15,** 326 (1998).
4. J. Primot, G. Rousset, and J. C. Fontanella, J. Opt. Soc. Am. A **7,** 1598 (1990).
5. H. J. Hofer, P. Artal, J. L. Aragón, and D. R. Williams, Invest. Ophthalmol. Visual Sci. Suppl. **40,** S365 (1999).
6. H. J. Hofer, P. Artal, B. Singer, J. L. Aragón, and D. R. Williams, "Dynamics of the eye's wave aberration," J. Opt. Soc. Am A (to be published).
7. P. M. Prieto, F. Vargas-Martin, S. Goelz, and P. Artal, J. Opt. Soc. Am A **17,** 1388 (2000).
8. W. K. Pratt, *Digital Image Processing*, 2nd ed. (Wiley, New York, 1991).